

FLUCTUATION AND MORPHOLOGICAL PROPERTIES OF THE PULSARS IN J0737–3039 SYSTEM

R. RAMACHANDRAN, D. C. BACKER, P. DEMOREST

Department of Astronomy, University of California, Berkeley, CA 94720-3411, USA

S. M. RANSOM¹, V. M. KASPI^{1,2}

Department of Physics, McGill University, Montreal, QC H3A 2T8, Canada

Draft version December 22, 2018

ABSTRACT

We describe the morphological and fluctuation properties of the pulsars in the double neutron star system, PSR J0737–3039. Pulsar **B** is seen in almost all orbital phases, except in the range of $\sim 6^\circ$ to 65° . This may be interpreted as an *eclipse* of pulsar **B**'s signal by its own magnetopause region produced by interaction with pulsar **A**'s relativistic wind. No modulation of the emission of pulsar **B** is found at the period of pulsar **A**. This places a constraint on the models that propose that pulsar **A**'s beamed radiation is directly responsible for pulsar **B**'s emission. Modulation index values indicate that the pulse to pulse variations in the two objects are mostly intrinsic. Pulsar **A** shows significant differential modulation index within its pulse profile.

Subject headings: pulsars: general – pulsars: individual (J0737-3039) – radiation mechanisms: non-thermal

1. INTRODUCTION

Recent discovery of the double pulsar system, reported by Burgay et al. (2003) and Lyne et al. (2004) is one of the most important discoveries in the history of pulsar astronomy. This high inclination system, which consists of a short period recycled pulsar and an ordinary slow pulsar revolving with an orbital period 2.45 hrs, gives us almost an ideal situation to probe many fundamental properties of neutron star astrophysics.

The distance between the two pulsars is so small (2.8 light sec), that the light cylinder volume (magnetosphere of a solitary pulsar) of PSR J0737–3039B (hereafter **B**) subtends about 20 degrees from PSR J0737–3039A (hereafter **A**).

It is unclear whether the measured value of \dot{P} of pulsar **B** is intrinsic to the pulsar, given the mechanical luminosity (\dot{E}) of pulsar **A**. It is conceivable that the relativistic wind from pulsar **A** influences the characteristics of pulsar **B**. In spite of this, pulsar **B** continues to emit radio radiation, clearly demonstrating the robustness of the fundamental radio emission mechanism. According to Lyne et al. (2004), this system may well have indicated that the seed acceleration responsible for this emission comes from deep inside the magnetosphere, clearly ruling out outer magnetospheric emission models.

The measured flux of pulsar **B** significantly changes as a function of orbital phase³ (Lyne et al. 2004).

Models have been proposed to suggest that the wind from pulsar **A** creates a magnetopause region around pulsar **B** due to the interaction with pulsar **B**'s magnetosphere (Arons et al. 2004). In this model, the synchrotron absorption optical depth of this magnetopause region is the primary reason for the observed eclipse of

pulsar **A**, and possibly for the light curve of pulsar **B**.

In this work, we present some of the basic morphological and fluctuation properties of these two pulsars. Section 3 describes the properties of average pulses of pulsar **A** and pulsar **B**. The fluctuation properties of the two pulsars are described in Section 4. Implications of our results are discussed in Section 5.

2. OBSERVATIONS

Observations were performed at the Green Bank Telescope (GBT) on 2003 December 11, 19, 23, & 24, and 2004 January 1. With the BCPM (Berkeley-Caltech Pulsar Machine; see e.g., Camilo et al. 2002), we observed at 430, 800, 1400 & 2200 MHz frequencies to record total power (Stokes-I parameter) at a time resolution of 72 μ sec. The bandwidths for the first two bands were 48 MHz (96 channels of 0.5 MHz each), and the last two were 96 MHz (96 channels of 1 MHz each). At 430 and 800 MHz, we also used the Spigot card with a bandwidth of 50 MHz.

The data was corrected for interstellar dispersion as part of our offline processing. We then added all channels together to produce a single time series. We used the ephemeris given by Burgay et al. (2003) for analysing the data from December 11th, 2003, and produced an improved ephemeris for pulsar **A**. This was then used for generating an ephemeris for pulsar **B** for all our subsequent observations.

3. PROFILE CHARACTERISTICS AND LIGHT CURVES

The two pulsars in this binary system show entirely different characteristics in their average properties. Apart from an eclipse of ~ 30 sec duration, pulsar **A** shows no significant variation in its light curve⁴, whereas pulsar **B** exhibits a spectacular orbital phase dependent variation in its light curve. Pulsar **A** shows significant average profile variation as a function of radio frequency which

¹ Center for Space Research, Massachusetts Institute of Technology, Cambridge, MA 02139

² Canada Research Chair, Steacie Fellow, CIAR Fellow

³ Orbital phase (ϕ_{orb}) is given as $(\omega + \eta)$, where ω and η are the position angle of periastron and the “true” anomaly.

⁴ Observed flux as a function of time

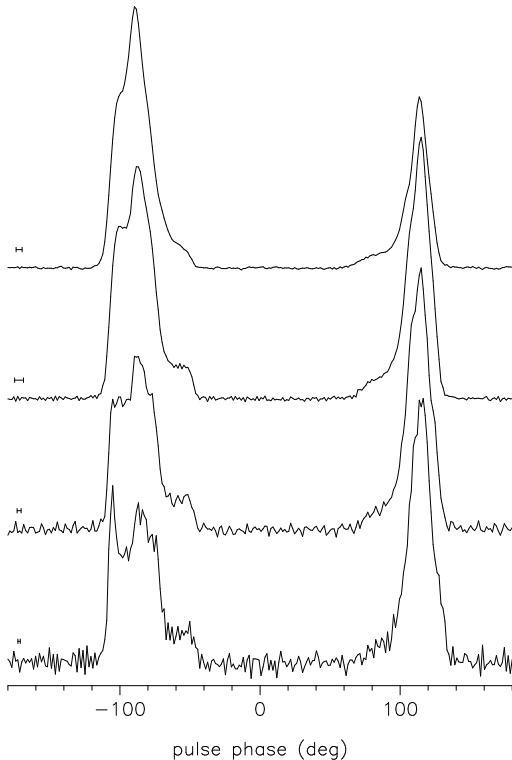


FIG. 1.— Average profiles of pulsar **A** at (top to bottom) 427, 820, 1400 & 2200 MHz. The profile at 427 MHz is from the SPIGOT card, and the rest are from BCPM. The effective time resolution for each of the profiles is indicated as a horizontal error bar. See text for details.

is seen in many other MSPs. Pulsar **B** shows significant profile variation not only as a function of frequency, but also as a function of orbital phase. We summarise all these properties in this section.

3.1. Average profiles of pulsar **A**

Pulsar **A** does not show any significant flux variation as a function of orbital phase outside of the eclipse region at its superior conjunction, whose characteristics are described by Lyne et al. (2004) and Kaspi et al. (2004). However, pulsar **A** shows considerable change in its average profiles as a function of radio frequency. We observed this pulsar at four different frequency bands, namely 427, 820, 1400 & 2200 MHz. Average profiles constructed from these data sets are given in Figure 1.

As Burgay et al. (2003) & Lyne et al. (2004) reported, we have a two-featured profile. Although these features appear like the classic main pulse and interpulse of an orthogonal rotator, the most favored configuration is likely an almost aligned rotation and magnetic axes, where our sight line cuts the emission cone in two different sides of the cone (Demorest et al. 2004). At the lowest frequency, the first feature is dominant, with less pronounced structures. However, at all the other frequencies, the second feature is dominant. Also, the first feature develops complex component structures. Although this is quite strikingly different from the behavior of ordinary long period pulsars, it is by no means uncommon among the shorter period pulsar population.

The amplitude reversal of components as a function

of frequency has been noted among several short period pulsars (millisecond pulsars). For instance, PSRs J0751+1807 & J2145-0750 are known to exhibit such reversal (Kramer et al. 1999). PSR J1022-1001 exhibits even a more complex evolution, where the component strengths reverse twice, while going from 400 MHz to a few GHz (Ramachandran & Kramer 2003). On the other hand, there are also counter examples like J0621+1002 & J1744-1134, where the pulsar exhibits little change in the profile structure.

We estimated the width and separation of the two features at all the frequency bands, and they do not seem to exhibit significant change. As it turns out, average profiles in all four bands could be fitted with seven gaussian components (4 for first feature, and 3 for the second). In order to quantify the profile span in longitude completely, we measured the width between the “base” (corresponds to approximately 1/50th of the peak value) of the raising and the trailing edge. This turned out to be 66° and 60° for the two features in all frequencies, and these values coincided within $2-3^\circ$. Similarly, the separation of the outer edges of the two features was $\sim 240^\circ$, and the separation of inner edges was $\sim 114^\circ$.

Several investigators have studied the variation of pulse width and component separation as a function of radio frequency. The classical ‘conal-single’ pulsars are known to exhibit a power law behavior, where the width of the pulse depends on radio frequency as ν^{-b} , where b is in the range of $\sim 0.1 - 0.3$ (Rankin 1983). Hankins & Fowler (1986) studied the frequency dependence of separation between the main and the interpulse of eight pulsars with interpulses. They find that although the main and the interpulse show considerable frequency dependence in their shape, the separation between them is frequency independent. Although this lack of frequency dependence tends to favor magnetic and rotation axes being almost orthogonal to each other (observed emission coming from both poles, with main pulse from one pole and the interpulse from the other pole: *two-pole model*), with their polarization observations, they point out that they favor the geometry where the two axes are almost aligned (*single-pole model*).

However, for recycled pulsars, the observed frequency dependence is more complex. The separation between the two features of PSR B1259-63 changes from $\sim 160^\circ$ to 139° while going from 660 MHz to 1.5 GHz. Then, at 4.7 GHz, the separation is 107° , and it stays constant above this frequency (Manchester & Johnston 1995). As Manchester & Johnston state, the most favored model for this pulsar is the single-pole model.

In the case of PSR J1022+1001, although the strength of the components evolve significantly as a function of radio frequency, and the profile itself shows significant instability over time scales of several minutes, the location of components and the width of the profile remains almost constant over a wide range of 328 MHz to about 4.8 GHz (Ramachandran & Kramer 2003). Kramer et al. (1999) present a very good summary of recycled pulsar profiles and their frequency evolution. In fact, their fig. 16 demonstrates clearly that the observed b values for recycled pulsars are very close to zero, with a few exceptions.

Therefore, one can conclude from the behavior of average pulses of pulsar **A** as a function of radio frequency

that it is no different from the general behavior of short period pulsar population. The lack of frequency dependence of either the pulse width or the main and the interpulse separation cannot be considered as a strong evidence for the two-pole model.

3.2. Light curves of pulsar **B**

As Lyne et al. (2004) indicate, pulsar **B**'s flux varies systematically as a function of orbital phase. In some phases, the pulsar is so bright that single pulses are detectable. However, in most of the orbital phase range, the emission is faint. Figure 2 shows that the pulsar is prominent in four orbital phase ranges (windows I to IV). For clarity, we have given the relative flux in logarithmic units and have repeated the light curve for two orbital periods. The inferior conjunction of pulsar **B** (when **B** is in front of **A**) occurs when $\phi_{\text{orb}} = 270^\circ$.

There are several features here that are noteworthy. Each sample in Figure 2 is produced by finding the area of the pulse after averaging some number of pulses. Owing to S/N considerations, we have taken unequal phase intervals for defining each sample in the plot. The shortest averaging length that we have taken is when the pulsar is very bright ($\phi_{\text{orb}} \sim 180^\circ$) where we have taken an average of 20 pulses. The longest length is when the pulsar flux was the weakest ($\phi_{\text{orb}} \sim 400^\circ$), where we have considered 700 pulses to find an upper limit to the average pulse flux.

It is worth emphasizing one important aspect of this light curve. In the orbital phase range of $\sim 6^\circ$ to 65° (modulo 360° in Figure 2), it appears that the pulsar signal exhibits what may be considered as an “eclipse”. We did not detect significant flux in this range at all. Although we cannot define the boundary of this “eclipse” region clearly due to signal to noise ratio considerations, the boundary appears to be very sharp. The physical mechanisms responsible for this behavior will be discussed in detail elsewhere (Arons et al. 2004).

Pulsar profiles reach a stable state only after averaging some thousand pulses (Helfand et al. 1975). Therefore, it is likely that our flux estimation in the phase ranges where we have taken very short averaging are somewhat in error. However, our emphasis here is on the overall systematic relative variations, and not on the absolute flux itself. As we will see in the next section, this behavior is not restricted to only the light curve, but also to the detailed profile structure.

There is some hint of chromaticity in the light curve during windows III and IV, where we observed lower flux at 1400 MHz than at 800 MHz. However, when the pulsar is bright, the light curve seems to be achromatic. A possible reason for the observed chromaticity in windows III and IV may be due to the line of sight passing close to the edge of the emission cone (impact angle β approximately equal to emission cone radius ρ), where the effective emission beam size is smaller at higher frequencies due to radius to frequency mapping.

3.3. Average profiles of pulsar **B**

In contrast to pulsar **A**, pulsar **B** shows significant change in its pulse profile structure as a function of orbital phase. For instance, the average profiles seen in window I are very different from those in window II. To demonstrate this effect, we have presented the average

profiles derived at three of our bands, 800, 1400 and 2200 MHz, in Figure 3. The orbital phase range corresponding to the four panels are given in the figure caption. The width of window I corresponds to approximately 830 seconds ($\sim 35^\circ$ of orbital phase – panels *Ia* to *Ic*). During this interval, the profile evolves significantly from having a slow rising edge (sharp trailing edge) to sharp rising edge (slow trailing edge). This is consistently observed in all the three frequencies. Although there are some differences in the average profiles in a given orbital phase range between one orbit to the next, these differences can be attributed to insufficient averaging in producing the average pulse.

In the fourth panel which corresponds to window II the profile displays two components, and these two components seem to be well separated at higher frequencies.

Among classical conal single pulsars, it is common to see profiles evolving into double profiles at lower frequencies. This is generally interpreted as due to radius-to-frequency mapping. Also, this model would certainly predict increasing width of the profiles with decreasing frequency. However, in the case of panel (*d*) (window II), the two components seem to be more pronounced with increasing frequency, which is the opposite of what we expect from radius-to-frequency mapping.

Having said this, it is also important to appreciate that in the case of the classical pulsar population, pulsars are solitary, and there is no influence on their magnetospheres from the surroundings. However, as Lyne et al. (2004) state, mechanical luminosity of pulsar **A** is significant enough to influence the magnetospheric properties of pulsar **B**. In fact, pulsar **B**'s proximity to pulsar **A** ensures that pulsar **B**'s magnetosphere is altered by pulsar **A**'s relativistic plasma wind.

There are three effects that can alter the emission amplitude and morphology of pulsar **B** (Demorest et al. 2004; Arons et al. 2004):

1. Orbital phase dependence of pulsar **A** wind pressure on pulsar **B**'s magnetosphere owing to the orientation of pulsar **A**'s magnetic and rotation axes.
2. Orbital phase dependence of the response of pulsar pulsar **B**'s magnetosphere to the pulsar **A** wind pressure, owing to the orientation and spin phase of pulsar **B** as we observe it.
3. Variable expansion of the pulsar **B** magnetosphere (at the spin phase of pulsar **B** when we observe pulsar **B**) into the downstream cavity created by the impinging pulsar **A** wind.

In all cases the variable magnetosphere shape will likely translate to variable polar cap size that, in turn, defines the active region of beamed radio emission which we parameterize with impact angle (β) and emission cone radius (ρ). While the effects in cases 1 and 2 are likely to produce rather small variations owing to the likely $P^{1/12}$ dependence of polar cap size on pressure, we expect that case 3 could lead to substantial variations.

4. FLUCTUATION PARAMETERS

It is well known that individual pulses from pulsars fluctuate in their intensity, location and shape, although the average pulse profiles of almost all pulsars show a

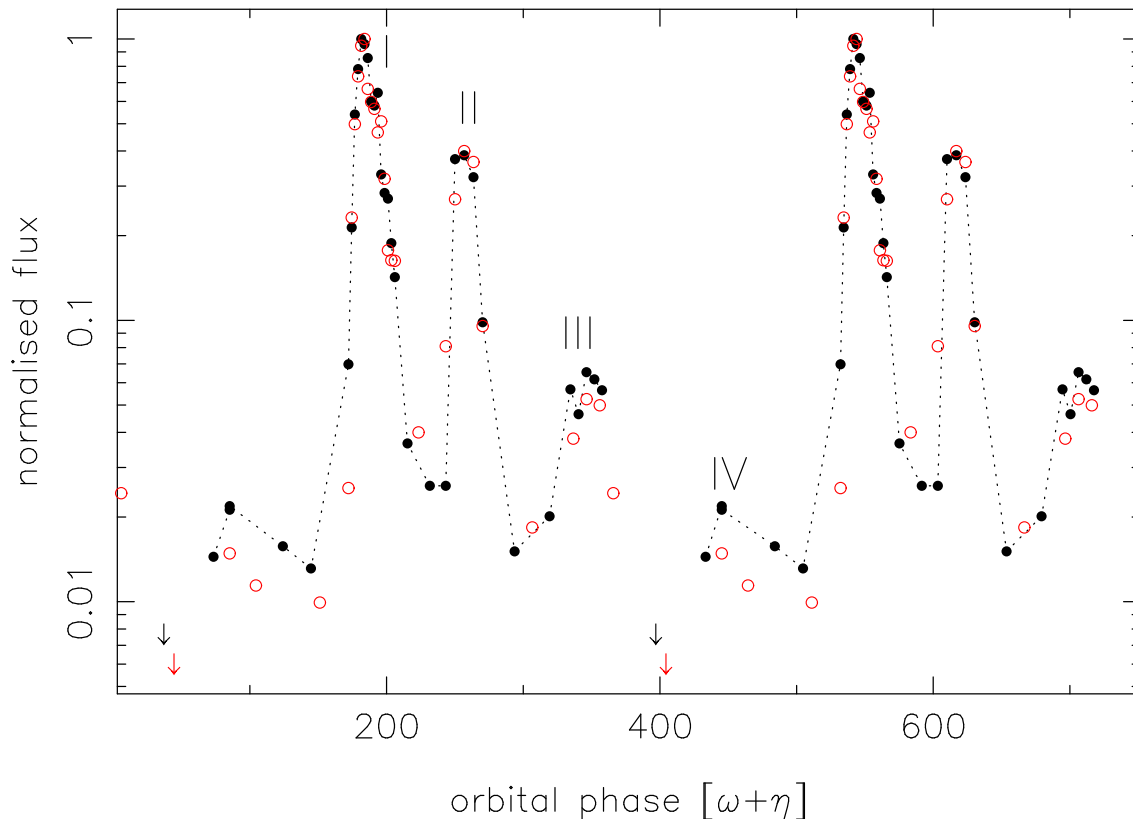


FIG. 2.— Light curve of pulsar **B** at 820 MHz (filled circles) and 1400 MHz (open circles). The four bright windows are indicated as I, II, III & IV. The dotted line has been drawn just for clarity. See text for details.

great deal of stability. These fluctuations exhibit a spectacular variety in their spectral characteristics. The intensity variations at a given pulse longitude are usually noiselike, although in many cases, there are quasi-periodic features. These quasi-periodic variations are usually associated with one of the most remarkable properties seen in pulsar signals – drifting subpulses. In this section, we will address various aspects of single pulse fluctuations seen in signals from pulsar **A** and pulsar **B**.

4.1. Modulation Index

One of the ways to quantify the amount of fluctuations seen in a given signal is by measuring modulation index, which is measured as

$$m = \frac{\sqrt{\sigma_{\phi}^2 - \sigma_o^2}}{\mu_{\phi}},$$

where σ_{ϕ} and σ_o are the variance seen in a given pulse longitude (ϕ) and the offpulse region, respectively; μ_{ϕ} is the mean flux measured at that longitude. With our 820 MHz data, for our analysis on pulsar **A**, we considered one hundred thousand pulses. In Figure 4, we give the measured modulation index as a function of pulse longitude. The left panel corresponds to pulsar **A**, and the middle and the right panels correspond to windows I and II of pulsar **B**. The measured value of modulation index comes to almost hundred percent across the pulse profile. That is, the r.m.s. variation in the flux level is as high as the mean level itself.

There are a few investigations reported in the literature that have measured intrinsic modulation index of pulsars. For instance, Weisberg et al. (1986) have measured modulation index values of many classical pulsars. They conclude that core components, on the average, have lower modulation index than the conal components. While the reason for this is not completely clear, perhaps it is due to a combination of intrinsic instability of conal component emissions of pulsars, and pulse nulling. As Rankin (1986) points out, pulse nulling has *never* been seen before in pulsars with only core emission. There is also a study of two MSPs by Jenet and his collaborators (Jenet & Gil 2004; Jenet et al. 2001). They conclude that PSR B1937+21 has very low – if not negligible – intrinsic modulation index, whereas PSR J0437–4715 exhibits a high modulation index. In general, it is unclear what the fluctuation properties of MSPs are when compared to ordinary pulsars, as no comprehensive study exists to date.

Interstellar scintillation is one well known source of extrinsic modulation that can contribute to the measured value of m . The expected value of m from the interstellar scintillation is given by $m_{\text{ism}} = 1/\sqrt{N_{\text{scint}}}$, where N_{scint} is the number of scintles in the band (Jenet et al. 2001). The observed modulation index is then given by $\sqrt{m^2 + m_{\text{ism}}^2}$. The value of N_{scint} is estimated as $N_{\text{scint}} = (1 + \eta B/\Delta\nu)$, where B is the bandwidth of observation, $\Delta\nu$ is the decorrelation bandwidth, and η is the packing fraction. The measured decorrelation band-

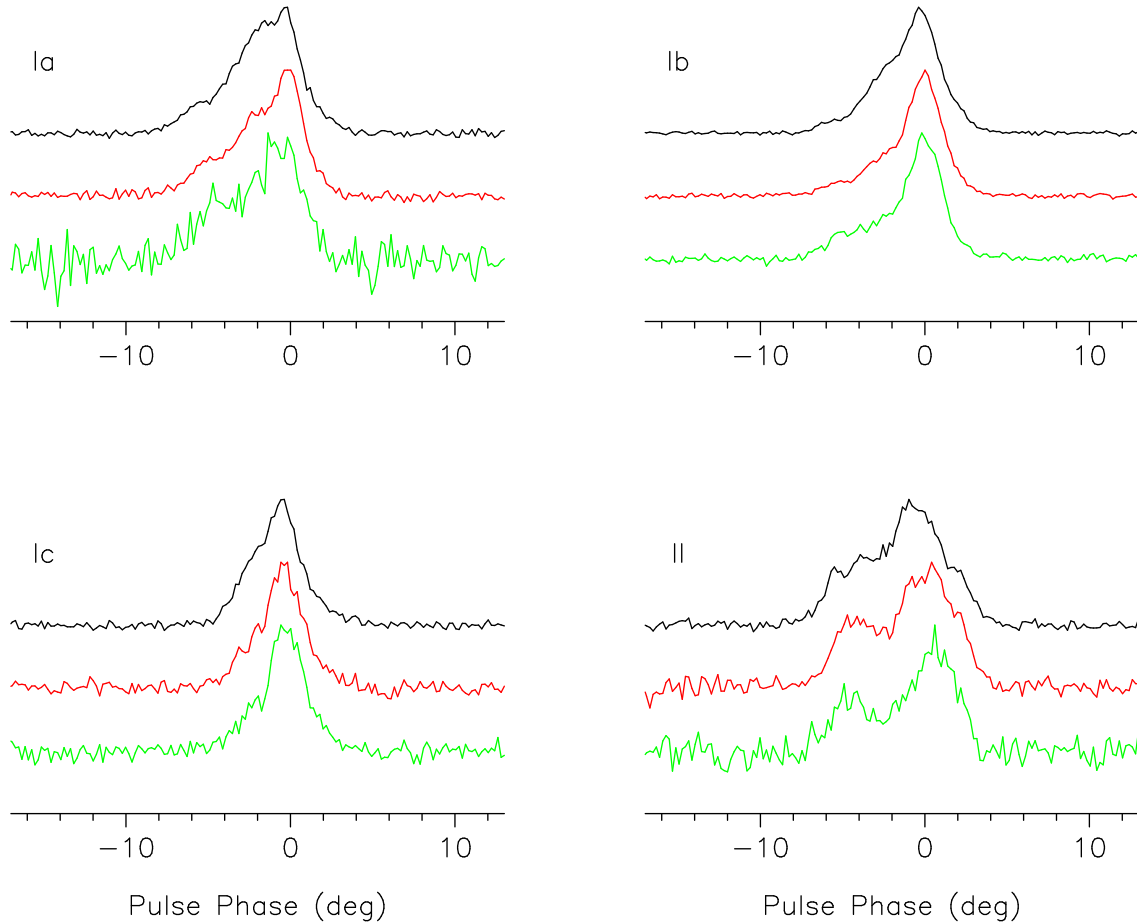


FIG. 3.— Average profiles of pulsar **B**. The four panels (Ia, Ib, Ic and II) correspond to orbital phase ranges of 171° – 183° , 183° – 195° , 195° – 207° & 240° – 273° , respectively. The three profiles in each panels are at 820 (top), 1400 (middle) and 2200 MHz (bottom), respectively. Pulse longitude given in the x-axis has arbitrary reference. See text for details.

width of pulsar **A** at 800 MHz is 0.1 ± 0.2 MHz, and at 1400 MHz is 1.8 ± 0.6 MHz (Ransom et al. 2004). Given the observed packing fraction of ~ 0.4 , the estimated modulation index due to interstellar scattering is about 7% at 800 MHz. In Figure 4, the inner regions of both features in the pulsar **A** profile seems to show significantly higher modulation index than the outer regions. Such variations in modulation index as a function of pulse longitude clearly suggests that there is certainly some intrinsic variation, and not all of it comes from the interstellar scattering. The high values of modulation index in the inner regions of the two features also possibly indicate that they are intermittent.

In windows I and II of pulsar **B**, although modulation index does not vary much as a function of pulse longitude, it seems to be much higher than what is expected from interstellar scattering. Therefore, we conclude that both the pulsars have significant intrinsic variability, whatever the spectral characteristics may be.

4.2. Fluctuation properties

Having established in §4.1 that pulsar **A** and pulsar **B** show significant intrinsic pulse fluctuation, we will assess the spectral nature of these fluctuations. For instance, these fluctuations could be almost fully associated with possible drifting subpulses as seen in many long

period pulsars. One of the ways to quantify these fluctuations is by computing the *longitude-resolved* (LR; Backer, Rankin & Campbell 1975) and *harmonic-resolved* (HR; Deshpande & Rankin 1999) spectra. In general pulsars show wide ranging spectral properties of pulse-to-pulse fluctuations, from very high coherence (like in the case of drifting subpulses in PSR B0943+10 & B0809+74 (Backer, Rankin & Campbell 1975; Deshpande & Rankin 2001 and references therein), or broad quasi-coherent features as in the case of PSR B2016+28. These (quasi-)coherent features not uncommon among pulsar population. All ‘conal-single’ pulsars are known to exhibit drifting subpulse phenomenon (Rankin 1986). Interestingly, highly coherent fluctuation features are seen in some components of ‘multiple-component’ pulsars like PSR B1237+25 (Backer, Rankin & Campbell 1975; Rankin & Ramachandran 2003). These coherent features are thought to represent some highly ordered kinematics in pulsar magnetosphere.

In the case of pulsar **B**, there is also another reason for looking for possible coherent intermodulations. Jenet & Ransom (2004) have recently proposed a scenario to explain the light curve of pulsar **B**. In their model, the near alignment of the magnetic and the rotation axes of **A** as suggested by Demorest et al. (2004) would mean

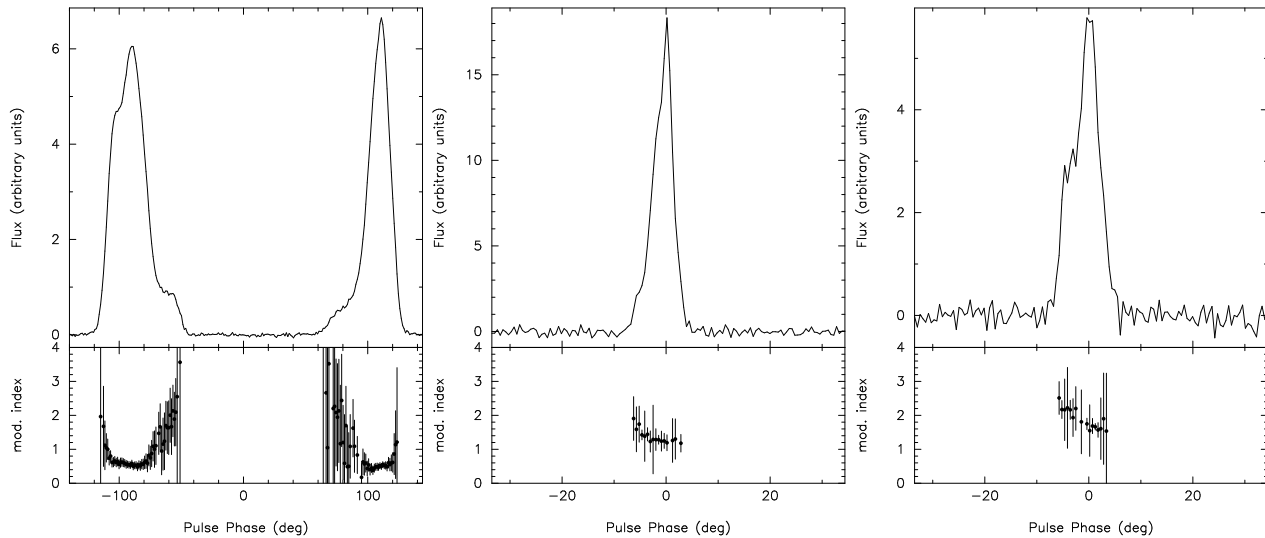


FIG. 4.— Modulation index (m) for pulsar **A** & pulsar **B**. (a) Upper panel gives average profile produced with five hundred thousand pulses of pulsar **A**. Modulation parameter is plotted as a function of pulse longitude in the lower panel. (b) & (c) give the same information for pulsar **B** in window I & II, respectively. Error bars indicate $1 - \sigma$ errors. The longitude resolution in all the plots have been chosen to optimize signal to noise ratio. See text for details.

that the emission cone of **A** is directed towards **B** in two phase ranges in the orbit. Then, if one assumes that pulsar **A**'s high energy emission is beamed the same way as the radio emission, then it is conceivable that the γ -ray emission from pulsar **A** influences pulsar **B**. They attribute the bright patches (windows I to IV) of pulsar **B**'s light curve to this direct influence from pulsar **A**.

If pulsar **A**'s beamed emission is directly responsible for pulsar **B**'s emission, then it is important to look for possible intermodulation between the two signals. That is, modulation of pulsar **B**'s signal with pulsar **A**'s periodicity. Since the rotation periods of these two pulsars are incommensurate with each other, if this modulation exists, it will manifest itself as *drifting subpulses* in pulsar **B**'s signal. Of course, this assumes that the environment of pulsar **B** does not influence the beamed radiation from pulsar **A** to reduce the effect of modulation. However, finding such a modulation will be a direct proof for such an interaction between the two pulsars.

The computed L-R and H-R spectra at 820 MHz and 1400 MHz failed to show any significant features in windows I & II, where we had adequate S/N. Owing to only a limited length of time in each window, we had only 256 pulses (~ 12 min). The corresponding spectral resolution in the LR spectrum is $(1/256P_1)$, and the spectral width is $(1/2P_1)$, where P_1 is the rotation period. Our sensitivity to detect any fluctuation feature was limited to one part in 540 in window I, and one part in 220 in window II.

We also looked for possible features in the LR and HR spectra of pulsar **A**. Although the possibility of having any influence of pulsar **B**'s radiation on pulsar **A** is low, pulsar **A** may have intrinsic spectral nature of its fluctuation properties that show (quasi-)coherent features in the LR and HR spectra. However, our analysis failed to reveal any such features within our sensitivity limit. Our sensitivity was one part in 3×10^4 , where we considered 500 thousand pulses for our analysis.

We conclude from these analyses that within our sensitivity limits, we do not detect any systematic intermodulation of the signals from pulsar **A** and pulsar **B**, and the intrinsic contribution to modulation index comes from fluctuations of broad spectral nature.

5. CONCLUSIONS

The measured flux from pulsar **B** shows systematic variation as a function of orbital phase. The pulsar is visible in all phase ranges except in the range of $\phi_{\text{orb}} \sim 6^\circ$ to 65° , where we have obtained only an upper limit to the flux. This void region may be interpreted as an *eclipse* of pulsar **B** by its own magnetopause region which is produced by interaction with the relativistic wind from pulsar **A**. It is this magnetopause region that may also be responsible for the eclipse of pulsar **A** around its superior conjunction (Arons et al. 2004). Although it is difficult for us to produce reliable light curve around this pulsar **B**'s apparent *eclipse* owing to signal-to-noise considerations, it is clear that the drop in flux is very rapid (within several pulses!)

With our observations at 800 and 1400 MHz, we see some indication of frequency dependence in pulsar **B**'s light curve. During windows III and IV, the flux at 1400 MHz seems to be systematically lower than the value at 800 MHz. This needs to be validated with further high signal-to-noise observations.

Modulation index measurements indicate variation of single pulse flux in both these objects. These variations are significantly more than what is expected from the measured decorrelation bandwidth (due to interstellar scattering) of this system. Therefore, these variations are intrinsic to the two pulsars. The inner regions in pulsar **A** seems to have significantly higher modulation index than the brighter outer regions.

Pulsar **A** exhibits a complex evolution of its average profile as a function of radio frequency. However, these properties do not seem to be different from the characteristics that short period pulsar population seems to

show.

Pulsar **B**’s profile shows dramatic variations as a function of orbital phase, making it impossible to solve for its geometric orientation without sensitive polarization measurements. The profile evolution as a function of frequency seems to reveal mainly a double component profile, where the components become more pronounced at higher frequencies. This is quite the opposite of what one would expect from simple dipole geometry, combined with radius to frequency mapping.

Given the possible geometrical orientation of pulsar **A** derived on the basis of polarimetric observations, it appears that there will be an orbital phase dependent wind pressure on **B** (Demorest et al. 2004). It is also plausible that the diameter of pulsar **B**’s emission cone changes due to the effect of orbital phase dependent pressure, thereby changing the fractional value of impact angle (β) with respect to the radius of the emission cone (ρ). This can introduce complex profile changes as a function of orbital phase, as we see for pulsar **B**. It is very important to understand the geometrical orientation of pulsar

B, for which sensitive polarimetric observations are necessary.

Within our sensitivity limits, there is no significant intermodulation between signals from the two objects. We do not detect any significant feature in the L-R & H-R spectra, indicating that the spectral characteristics of the intrinsic pulse fluctuations is “noiselike”. This constrains the models proposing direct influence on the emission mechanism of pulsar **B** by radiation from pulsar **A**.

We thank the GBT staff, and in particular Carl Bignell, Frank Ghigo, Glen Langston and Karen O’Neil, for extensive help with the observations and very useful discussions. V.M.K. is supported from NSERC Discovery Grant 228738-03, NSERC Steacie Supplement 268264-03, a Canada Foundation for Innovation New Opportunities Grant, FQRNT Team and Centre Grants, and the Canadian Institute for Advanced Research. V.M.K. is a Canada Research Chair and Steacie Fellow. RR would like to thank A. A. Deshpande for valuable discussions.

REFERENCES

- Arons, J. A., Spitkovsky, A., Backer, D. C., Kaspi, V. M. 2004, ApJ, in preparation
- Backer, D. C., Rankin, J. M., Campbell, D. B. 1975, ApJ, 197, 481
- Backer, D. C., Wong, T. & Valanju, J. 2000, ApJ, 543, 740
- Burgay, M., D’Amico, N., Possenti, A. et al. 2003, Nature, 426, 531
- Camilo, F., Stairs, I. H., Lorimer, D. R. et al. 2002, ApJ, 571, 41
- Demorest, P., Ramachandran, R., Backer, D. C., Ransom, S. M., Kaspi, V. M., Arons, J., Spitkovsky, A. 2004, ApJ, Submitted (astro-ph/0402025)
- Deshpande, A. A. & Rankin, J. M. 1999, ApJ, 524, 1008
- Deshpande, A. A., Rankin, J. M. 2001, MNRAS, 322, 438
- Jenet, F. A., Gil, J., 2004, ApJ, 602, L89
- Jenet, F. A., Anderson, S. B., Prince, T. A. 2001, ApJ, 546, 394
- Jenet, F. A., Ransom, S. M. 2004, Nature, in press
- Hankins, T. H., Fowler, L. A. 1986, ApJ, 304, 256
- Helfand, D. J., Manchester, R. N., Taylor, J. H. 1975, ApJ, 198, 661
- Kaspi, V. M., Ransom, S. M., Backer, D. C., Ramachandran, R., Demorest, P., Arons, J., Spitkovsky, A. 2004, ApJ, Submitted (astro-ph/0401614)
- Kramer, M., Lange, C., Lorimer, D. R. et al. 1999, ApJ, 526, 957
- Lyne, A. G., Burgay, M., Kramer, M., Possenti, A., Manchester, R. N., Camilo, F., McLaughlin, M. A., Lorimer, D. R., D’Amico, N., Joshi, B. C., Reynolds, J., Freire, P. C. C. 2004, Science, 303, 1153
- Manchester, R. N. & Johnston, S. 1995, ApJ, 441, L65
- Ramachandran, R. & Kramer, M., 2003, A&A, 407, 1085
- Rankin, J. M. 1983, ApJ, 274, 359
- Rankin, J. M. 1986, ApJ, 301, 901
- Rankin, J. M., Ramachandran, R. 2003, ApJ, 590, 411
- Ransom, S. M., Kaspi, V. M., Ramachandran, R., Demorest, P., Backer, D. C., Pfahl, E. D., Ghigo, F. D., Kaplan, D. L. 2004, ApJ, submitted (astro-ph/0404149)
- Weisberg, J. M., Armstrong, B. K., Backus, P. R., Cordes, J. M., Boriakoff, V., Ferguson, D. C. 1986, AJ, 92, 621